Digest Journal of Nanomaterials and Biostructures Vol. 11, No. 2, April - June 2016, p. 663 - 674

GROWTH OF ZnO NANORODS BY TWO-STEP SOLUTION PROCESS FOR ETHANOL AND HYDROGEN GAS SENSING AT LOW TEMPERATURE

M. JABEEN[a*], M. A. IQBAL[b], M. T. JAVED[c], N. ALI[d], M. AHMED[a], R. ALI[d], S. SARFRAZ[e], R. V. KUMAR[e]

[a] *Department of Physics University of the Punjab Lahore, Pakistan*
[b]*Department of Physics University of Management Technology Lahore*
[c]*Department of Chemical Engineering, Pakistan Institute of Engineering and Applied Sciences, Nilore, Islamabad, Pakistan*
[d]*Department of Physics, Faculty of Science, University Technology Malaysia*
[e]*Department of Material Science and Metallurgy, University of Cambridge United Kingdom*

ZnO nanorods were grown by 2-step solution process. The seeding layer was prepared by thermal de-composition of zinc acetate di-hydrate at a temperature of 150^{o}C for 1 h and then ZnO nanorods were synthesized from a solution of $Zn(NO_3)_2$. The seed layer increase the nucleation during the growth by hydrothermal process but ZnO growth without seed layer is random in rod shape. The synthesized ZnO nanorods were found to have hexagonal wurtzite structure with good aspect ratio. The characterization of nanorods was carried out by X-ray diffraction, field emission scanning electron microscope and UV-visible spectroscopy. The experimental results on ZnO nanorods synthesized by hydrothermal process used for ethanol gas sensing are reported at low temperature from 50-80^{o}C, in the presence of humidity at different gas concentrations 10, 20, 50 and 100 ppm. We also investigate the humidity level from 30-50 at a temperature range from 50-80^{o}C in the present study. The response (%) of 50 ppm of ethanol at a fixed temperature of 80^{o}C verses time showed the same repeated values. The 100 ppm hydrogen gas detection was performed at various temperatures and sensitivity was observed highest at 50^{o}C. Gas detection was carried out at lower temperature as compared to reported in the literature for the very first time. ZnO nanorods structure have diameter in the range of 100-150 nm and length more than 1μ as determined by FESEM. In addition, it was suggested from UV-visible spectroscopy that as grown ZnO nanorods has good absorption spectrum.

(Received May 6, 2015; Accepted June 17, 2016)

Keywords: ZnO nanorods, Ethanol sensor, Hydrothermal process, Hydrogen sensor, Sol-gel process

1. Introduction

Semiconductor metal oxide nanostructures have great attraction in gas detecting devices due to their appealing properties and potential applications. [1] Nanostructures have high aspect ratio that is imperative for quick response and rapid diffusion of gases in the sensing area. [2]

Semiconductor 1-D nanostructures such as nanowires, nanorods, nanotubes and nanobelts have much attention for researchers due to their exceptional properties. [3] Zinc oxide (ZnO) is intrinsically an n-type material with wurtzite structure that is favorable for conducting devices. ZnO belongs to II-VI semiconductor materials having wide direct band-gap 3.37 eV and large value of exciton binding energy (60 meV). [4, 6] ZnO has exceptional properties in the field of electronics and optoelectronics. Therefore it has been extensively explored for technological purposes like solar cell, light emitting diodes, piezoelectric transducers and gas sensors. [7-10] In literature, ZnO sensors are reported for H_2, CO, O_3, NH_3, NO_2, acetone and ethanol sensing.

* Corresponding author: musarrat95@hotmail.com

Generally, in semiconductor oxides gas sensing depends on surface morphology. Usually a sensor has high aspect ratio that is fabricated at nanometer scale.

To design highly selective, sensitive, compact and reliable detecting devices to sense toxic, chemical, biological and flammable elements is of great importance.[11] Gas sensors based on semiconductor metal oxide are preferably used for emission and environmental monitoring, domestic, automotive, medical and in industrial applications. These gas sensors have advantages like small size, cost effective and inertness. The gas detection mechanism of such sensors depends upon oxygen chemisorptions on the oxide surface. [12] During reactions with oxygen and gases, molecular charge is transferred. Corresponding to gas concentration the conductivity and carrier density changed. [13-16] Gas sensing mechanism is totally a surface phenomenon which related surface to volume ratio, porosity and granularity.

Several methods have been reported to synthesized ZnO nanorods, including sol gel method,[17, 18] metal organic chemical vapor deposition (MOCVD), radio frequency (RF) magnetron sputtering [19] medium frequency magnetron sputtering.[20] DC magnetron sputtering,[21] pulsed laser deposition, and spray pyrolysis etc.[22] Unfortunately, above techniques demands high cost, hard conditions for reaction mechanism and small selectivity for the impurities. In comparison, hydrothermal fabrication of ZnO nanorods by thermal decomposition of zinc acetate dihydrate [$Zn(CH_3COO)_2.2H_2O$] features a simple and economical process that used easily available raw materials.

Moreover, hydrothermal technique can be easily controlled. These advantages make the technique best for the growth of ZnO nanorods. [23] The hydrothermal technique includes a number of processes, involving dissolution, hydrolysis, generated mixture, crystallization and polymerization. In ethanol solution $Zn(CH_3COO)_2.2H_2O$ was dissolved and breaks down under heating environments to produced ZnO layer,[24-28] as mentioned below:

$$Zn\ (CH_3COO)_2.2H_2O \rightarrow 2CH_3COOH \uparrow + ZnO + 2H_2O \uparrow$$

Ethanol monitoring is essential in some chemical industries as well as for drivers to check alcohol levels. ZnO, SnO_2 and different other oxides are widely explored for their sensitivity to ethanol. Likewise hydrogen becomes "the universal fuel for the future" due to its estimated successor of the hydrocarbons. Hydrogen is orderless, invisible and combustible gas. It is crucial to design hydrogen sensors for its transportation and hydrogen engine cars. [27]

In this research we had developed a cost effective, simple and rapid synthesis technique for fabrication of ZnO nanorods by thermal decomposition of zinc acetate di-hydrate at 150^{o}C in an air atmosphere. The characterization of ZnO nanorods were carried out by X-ray diffraction (XRD), field emission scanning electron microscopy (FESEM) and absorption.[29, 30] The experimental results of ZnO nanorods synthesized by thermal decomposition process used for ethanol and hydrogen gas sensing at low temperature are also reported in this study.

2. Experimental details

2.1 Preparation of solution

Zinc acetate 2-hydrate ($Zn\ (CH_3COO)_2 \cdot 2H_2O$, 99.5% purity Sigma Aldrich U.K) was used as starting precursor. Absolute ethanol and di-ethanolamine (DEA, $HN\ (CH_2CH_2OH)_2$) were used as solvent and solution stabilizer. We prepared a 0.5 M ZnO solution by mixing 0.05 mol of zinc acetate 2-hydrate in 0.1 litter of ethanol. Mixture was taken in a 250 mL glass beaker and stirred for half an hour. During continuous stirring DEA was added drop wise into the solution mixture. The molar concentration was adjusted at 1 of DEA/$Zn2^{+}$. After continuous stirring for 30 min the solution became homogenous and clear. Before the use for final coating, the solution was stirred continuously overnight.

2.2 Growth of seed layer

By spin coating a seed layer of 300 nm thick was prepared on a substrate. Prior to seed layer deposition, the substrate cleaned with distilled water (18 MΩ), isopropyl alcohol,

ultrasonicated for 30 min. in acetone, then rinsed with deionized water and dried in nitrogen atmosphere. The seed layer was produced by spin coater with a speed 20 rpm, acceleration = 1500 m/s^2, t = 15 s and have a thickness 50 nm. After each spin coating, seeding layer was directly dried on hot plate at a temperature of 40^{o}C for 5 minutes. To attain a desired thickness of 300 nm, we repeated this procedure six times. The post annealing was carried out in a furnace for 1 hour at a temperature of 120^{o}C with heating rate of 10^{o}C/min.

2.3 ZnO nanorods manufacturing

By the hydrothermal process ZnO nanorod arrays synthesized on the as prepared seed layer. The prepared seeding was washed with deionized water to remove the impurities. Prepared 0.01M growth solution of Zn $(NO_3)_2$ in deionized water adjust its pH 10 with NaOH and stirred the solution at 75^{o}C for 2 h. These seeding substrates suspending inverted in the nucleation solution for 12 h and changed the solution for every 4 h for the better growth of nanorods.

The crystal pattern was evaluated with X-ray diffraction (XRD, Buruker D8 Advance) using Cu Kα = 0.154 nm radiation at 40 kV and 40 mA current. Surface morphology of thin film was determined by SEM (JEOL-6340F). Optical properties were examined with a UV/Vis spectrophotometer (Lambda 750).

3. Results and discussion

3.1 Crystal structure and surface morphology

To investigate the crystal pattern of the ZnO nanorods, we used the crystalline and drying phenomenon of the precursor. Normally, for processes such as oxidation and drying the heat treatment is necessary. The wet precursor of zinc acetate crystallizes by the following reactions. [31, 32]

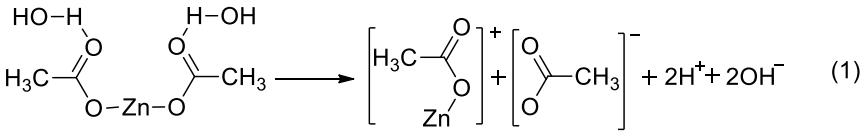

(1)

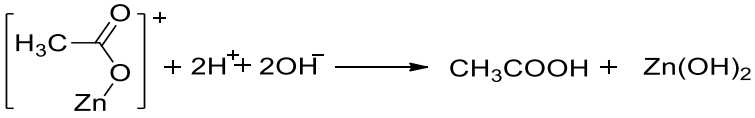

(2)

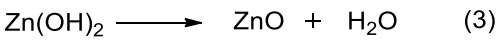

(3)

The wet precursor thin film crystallized through the thermal de-composition of the containing molecules. Actually, while drying an acetic acid order was investigated that confirm the release of acetic acid as mentioned in equation (2). When the heat treatment temperature was less than 120^{o}C due to remaining organic compound one could not attain transparent ZnO nanorods thin film. As reported earlier [17, 18] that organic compound present on the ZnO surface should be dry and burnt at 150^{o}C. The XRD pattern (Fig.1) showed hexagonal structure. However, no peaks of other mineral or diffraction of Zn $(OH)_2$ were investigated that confirmed the purity of ZnO nanorods. Consequently, crystalline structure improved with temperature. The XRD pattern represents that a=b=3.2499 nm, α=β=90^o, γ=120^o, these parameters are according to standard card No. [JCPDS card no. 01-079-0206 having space group: P63mc (1997)]. The peak with 100 % intensity appears at 2θ = 36.26 with indices (k h l) = (1 0 1), 2nd peak appears at 2θ = 31.8 with indices (k h l) = (1 0 0) have 57 % intensity and the third main peak appears at with 2θ = 34.4 having indices (k h l) = (0 0 2) with intensity 41.4 %. Due to back scattering radiations the other peaks lies in various planes. As nanorods have not any precise direction that is confirmed from indices. They are randomly oriented. No impurity peaks were detected.

The surface morphology was investigated with SEM as indicated in fig. 2. The SEM images (a), (b), (c) and (d) taken at magnifications 11,000, 55,000, 18,000 and 17,000 etc. All the images have the same format JEOL/EO taken by the instrument JSM6340F with accelerating voltage 30 kV, Signal SEI, WD = 9 and at mood standard.

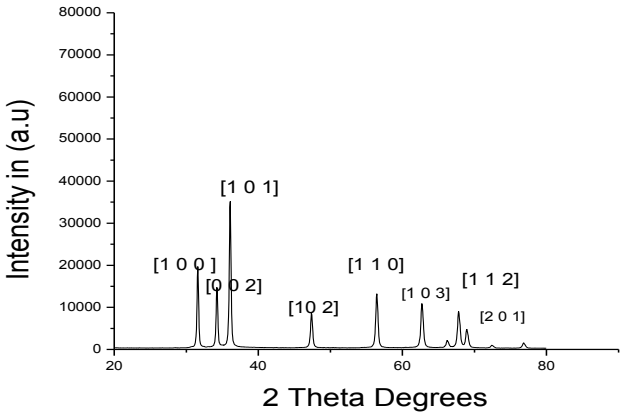

Fig.1 XRD analysis of ZnO nanorods grown by thermal decomposition technique

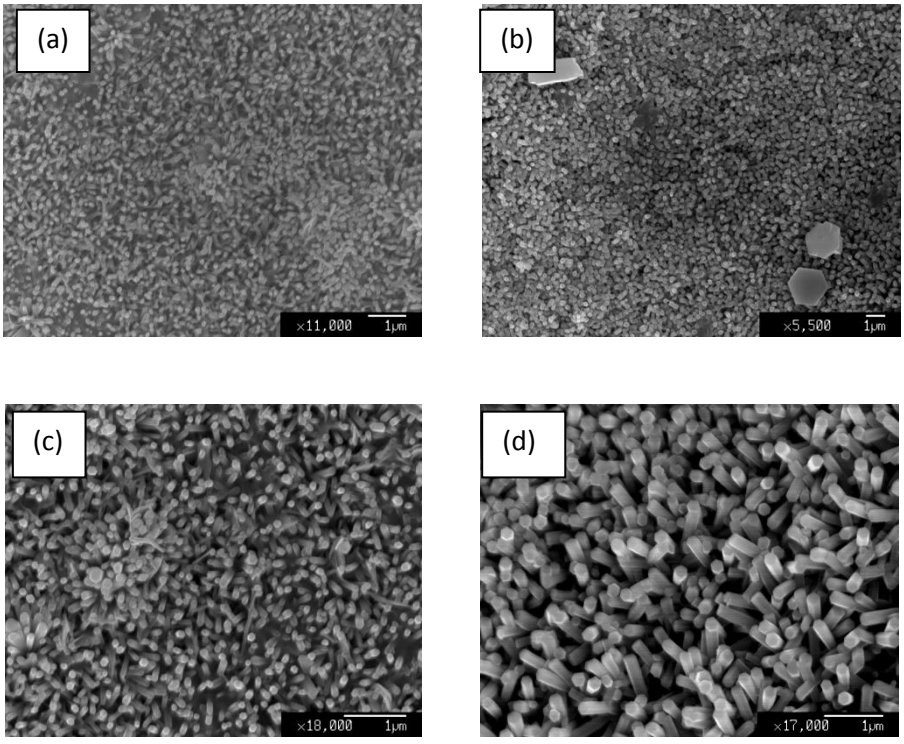

Fig.2. Surface morphology of the ZNO nanorods at different magnifications

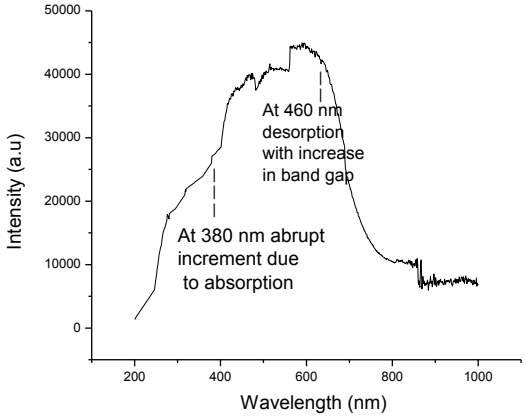

Fig.3. Absorption study of ZnO nanorods prepared by thermal decomposition method

3.2 Optical properties

The optical absorption spectrum of ZnO nanorods fabricated by thermal decomposition process is shown in Fig. 3. The absorption spectra have abrupt increase at 380 nm wavelength annealed at 150^{o}C in air. The fluctuations are due to interference phenomenon so absorption decreases. At higher temperature the grain sizes enhanced by crystallization. However, coherence between primary and reflected light beam lost at film boundaries due to scattering. Hence, the transmittance reduces by disappearing in interference fringes [33].With increase in temperature the absorption edge was high which indicates decrease in band gap. ZnO nanorods show an abrupt increase in intensity at 380 nm wavelength. The intensity of nanorods fluctuates between 380-650 nm then there is fall in the intensity till 800 nm. This study shows that ZnO nanorods have good absorption ability. The results are in agreement with the reported data regarding optical properties of ZnO nanorods. [28]

Gas absorption will also influence the luminescence property of ZnO Nanorods. The resistance reduces with the exposure of light and depletion of nanorods layer. The sensor indicates a greater resistivity as an electron from the conduction band adsorbed by O_2 molecule. ZnO Nanorods absorb radiation when a photon is more energetic than the Eg (band gap) energy, thus an electron hole pair is generated. The photo created holes counterbalanced the chemisorbed O_2 executive for greater resistance, enhancing the conductivity of the sensor. As a result, the conductivity in the sensing material enhanced brings about photo-current [34]. The gas absorption also influences the luminescence property of ZnO nanorods.

3.3 Gas sensing properties

Gas response in terms of resistance was measured by a digital multimeter attached with the gas test chamber. Dry air passed through the gas test chamber and mixed with desired concentration of ethanol. Ethanol (detecting gas) mixed with air when flowed through the gas chamber.

Generally, the gas detection mechanism depends upon the adsorption and desorption of the test gas that proposed on reversible chemisorptions of C_2H_5OH on ZnO nanorods surface. Depletion length changed due to production of reversible variation in resistivity between ZnO surface and ethanol with the exchange of charges.

Gas sensing properties were calculated by Keithley multimeter-614, mass flow controller and a home-designed gas test chamber. The hydrogen and ethanol vapors were tested by the sensor in the range of temperature 20-80^{o}C. Adjust the gas flow at 100 sccm with mass flow controllers. The operating temperature was maintained with a hot-plate.

In a normal operation, to enhance the sensitivity sputter a thin film of Pt on the sensing surface of 2×2 area. We put the sensor in a detecting chamber at room temperature. Then a suitable quantity of ethanol is injected in the chamber. The variation in resistance (conductivity) of the gas sensor was monitored with a digital Keithley-614 electrometer. Evaluate the ethanol sensitivity corresponds to active sites of ZnO nanorods surface fabricated by 2-step solution method. The

sensor behavior depends upon temperature and the resistance characteristics in dry and humid air. The experimental results reveled that by increasing the operating temperature there was a reduction in the resistance of the sensor due to intrinsic property of the semiconductor materials. The oxygen adsorbed on the surface converted into ions of oxygen by free electrons capturing (O^-, O_2^-, O^{2-}). Chemically the O_2 atoms adsorbed on ZnO surface and in the presence of temperature reaction take place as follow.

$$O_{2\,(ads)} \leftrightarrow O_{2\,(ads)}^{-} \leftrightarrow 2O^{-}_{\,(ads)} \leftrightarrow 2O_2^{-}{}_{(ads)} \quad \text{(a)}$$

When O_2 adsorbed on the surface conduction band provide free electrons and O_2 ions are given by equation. [35]

$$O_{2\,(ads)} + 2e^{-} \rightarrow 2O^{-}_{ads} \quad \text{(b)}$$

The carrier concentration reduced due to formation of depletion region on the surface. Ethanol acts as reducing gas. When ethanol vapor flowed on the surface of the sensor will interact with O_2 ions. The reaction is as under:

$$C_2H_5OH + 6O^{-}_{(ads)} \rightarrow 2CO_2 + 3H_2O + 6e^{-} \quad \text{(c)}$$

The electrons released in the conduction band so current in the sensor will increase. In air the depletion width is normally several nm. The diameter of nanorods is greater than the width of depletion layer. The depletion width has effect on the mobility and density of the es^- in the nanorods surface. The current of the sensor was controlled by the energy barrier contact. The sensor response curve between the resistance and temperature represents a decrease in the resistance.

Normally, we assume that by introducing ethanol the current increases due to small contact barrier between the nanorods and silver electrodes. It is due to the possibility that diffusion take place from ethanol vapor to Pt metallization (a metal layer was coated on substrate by metallization procedure which provide electrical connection to the sensor) and nanorods surface, thus the contact barrier decreases. Thus many electrons transport in the sensor due to that mobility and density of the carrier increases. The reaction supplied enough electrons as a result resistance of the nanorod sensor decreases.

Current is transported by conduction band es^- in the n-type semiconductor metal oxide sensors. At grain boundaries adsorbed atmospheric oxygen captured by the electron carriers. The resistance decreases upon exposure of ethanol due to reaction between –ve charge oxygen and reducing gases then occupied electrons are released by the reactions. [36]

Actually, the sensitivity and specific area influenced the energetic sites of the surface of the material. The adsorbed gases and oxygen can be detected by active sites. Accordingly, high gas sensitivity corresponds to greater oxygen adsorption quantity and specific surface area of the material. The sensitivity can be defined in various forms; here we have it a ratio of as ($S = R_{air}/R_{gas}$. The defects formed during fast growth of nanorods. For gas quickly diffuse into nanorod sensor from outer surface by holes and channels.

Moreover, the gas detected as well as penetrated into the material of the sensor by means of holes and channels that contact with the inner surface of the sensor. Consequently, a greater surface area obtained. However, for diffusion of air molecules defects are helpful and the resistance of the sensor enhanced by trapping electrons from oxygen.

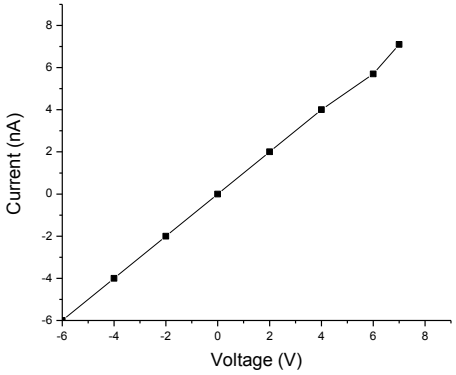

Fig.4 I-V characteristics of the ZnO nanorod sensor in air

Fig.4 represents current voltage characteristics measured by Keithley 614 electrometer in air. It has been observed that there is linear relationship between current and voltage. This indicates that a good ohmic contact is form. A representation of the sensing measuring device is shown in Fig. 4 (a).

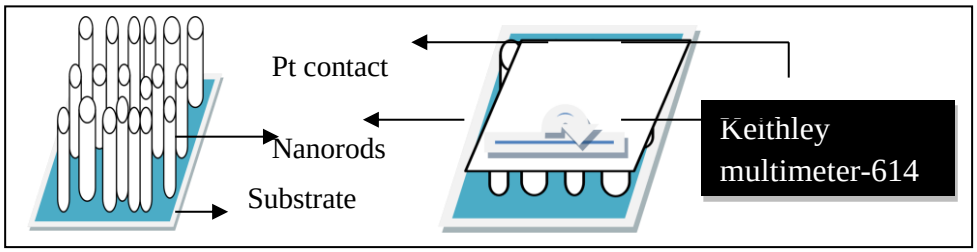

Fig.4 (a) Schematic diagram of the ZnO nanorods arrays

The gas sensor fabricated by the as frown ZnO nanorod arrays not by a single nanorod on the conducting substrate. The contacts are applied on the upper surface of substrate and ZnO Nanorods after sputtering a thin layer of Pt to enhance the conductivity and then connecting wires with silver paste.

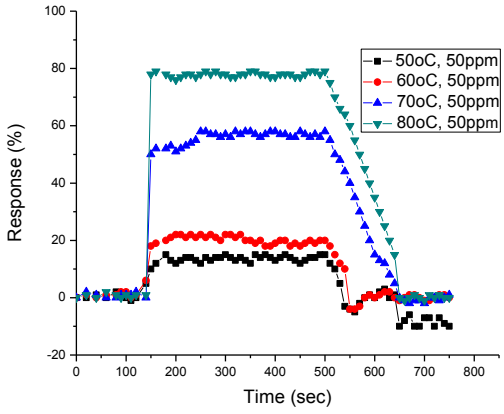

Fig.5 Response of ZnO nanorods to 50 ppm ethanol at different temperatures

During the response measurement the environmental humidity was 50% at room temperature 25^{o}C. We measured the sensor resistivity in air (R_a), then ethanol gas of 50 ppm

concentration was allowed to flow in the chamber. In the presence of ethanol the resistivity of the sensor was measured (R_g). The response is defined as [$((R_a-R_g)/R_a) \times 100\%$]. The measured values of responses were 50 and 75% when sensor was operated at 70°C and 80°C respectively. The response increases with temperature due to intrinsic property of semiconductor materials.

The sensing process is a surface controlled phenomenon. In sensing ethanol the oxygen portion is significant in measuring electrical transportation characteristics. The conduction electrons removed by O_2 iono-sorption. Hence it slows down the conduction of ZnO nanorods. It was reported by Barsan et al. [38] that the reaction between atmospheric oxygen.

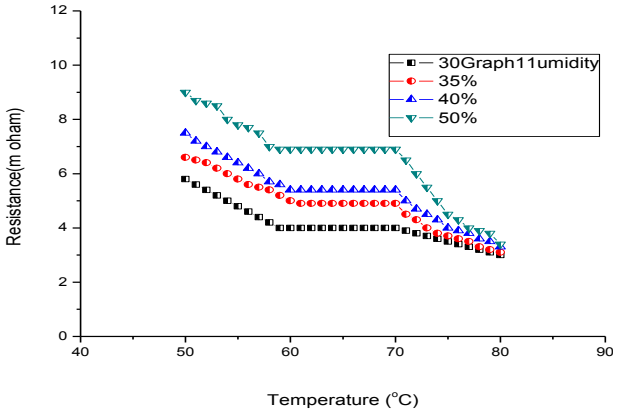

Fig. 6 Resistance of the sensor at different humidity levels from 30-50% measured at different operating temperatures from 80-200°C.

Fig.6 shows the resistance of the sensor can be measured as a function of relative humidity in the range 30 to 50% at different temperatures. The resistance depends on humidity. At constant temperature with increase in humidity resistance decreases. [37] It has been verified from Barsan et al. [38] that water vapor support to enhance the conductivity of the semiconductor. The affect of water vapors by means of specific surface area plays an important role. The adsorption of water vapor also enhance by the surface defects. Since ZnO is an n-type material at fixed humidity level, with increase in temperature resistivity decreased in nanostructure of ZnO due to the generation of electron hole pairs. Resistance has highest value with different humidity levels at 50°C varies from 5.8-9 MΩ. Moreover, at 80°C the resistance values have the same approach at different humidity values. The smallest value of the resistance measured was 3 MΩ. Hence, resistance fluctuation decreased by the water vapors at 80°C.

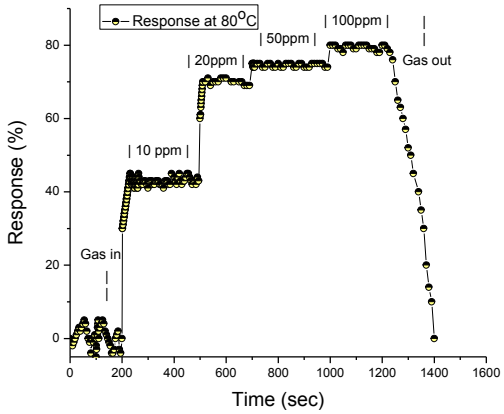

Fig. 7 Response of ZnO nanorods sensor to ethanol as a function different concentration of gas

All measurements were made at 80°C with different concentrations of ethanol. When the concentration of ethanol was 10, 20, 50 and 100 ppm the corresponding values of responses were 45, 70, 75 and 80 %. It was concluded from experimental results that with the increase in ethanol concentration the response enhanced.

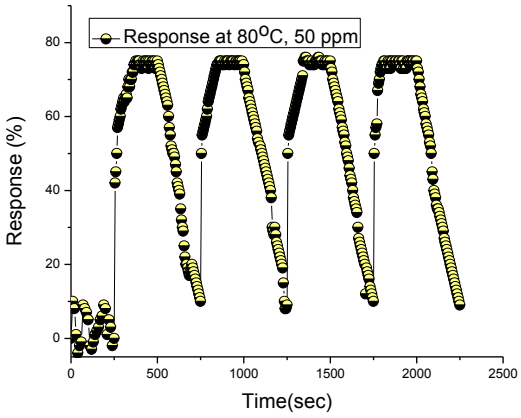

Fig.8 Reproducible response to ethanol by ZnO sensor at 80°C

The sensor responded rapidly to ethanol at 80°C. The plots show that sensor has stable response (%) and recovery time at 50ppm of ethanol.

Moreover, the sensor in the hydrogen environment operate in the adsorption desorption detection mechanism and investigated on the reversible chemisorptions of gas on ZnO nanorod exposed area. Reversible change in resistance happens due to transfer of charges between the ZnO surface and hydrogen gas which accelerate to the change of depletion width. The current enhanced in Nanorods due to release of electrons from conduction band as explained below:

$$H_2 + 1/2\ O_2^- \rightarrow H_2O + e^- \quad \text{(a)}$$

$$H_2 + O^-(ad) \rightarrow H_2O + e^- \quad \text{(b)}$$

The H_2O molecules produce by the reaction of absorbed oxygen ions and H_2 molecules. The current enhanced through nanorods due to discharge of electrons and hence the depletion width decreases. The exothermic reaction (1.8 kcal mol^{-1}) and water desorbed from the surface. The gas response and reaction among H_2 and O_2 ions are responsible for greater no of oxygen ions on the surface of ZnO nanorods. [39, 12] The experimental results investigated that the diameter of ZnO nanowires, their aspect ratio and depletion layer contribute majorly in the sensing phenomenon. [15]

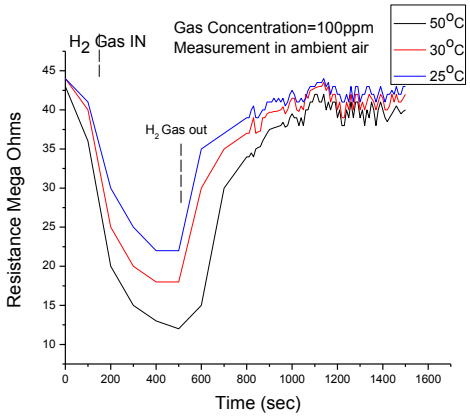

Fig. 9(a) Resistance of hydrogen gas versus time at various temperatures

The experimental results shows that resistance of the sensor decreased with the flow of hydrogen gas and with the increase of working temperature sensitivity of the sensor enhanced. The resistance attains a value of 12 MΩ in 500 s after that it gains approximately original value. In the time interval between 0-500 s the decrease of resistance with time is in 15 s. When the hydrogen gas is cut off from the gas chamber the resistance begins to increase with approximately in the same interval of time but after 800 s, resistance change is very small. We have measured resistance change up to 1600 s that is in fraction. So curves are much closer together.

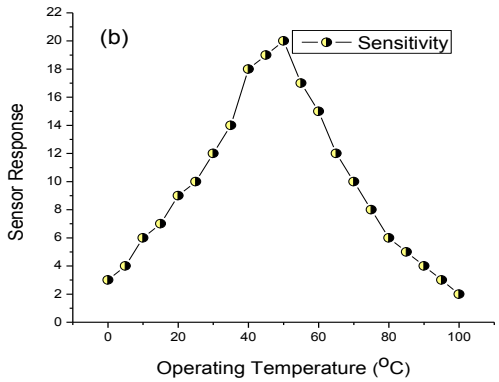

Fig. 9(b) Sensitivity of ZnO nanorods at different operating temperatures

The sensitivity of the sensor enhanced with the operating temperature and maximum attained at 50°C and then it gradually decreased.

4. Conclusion

This research reports the high purity ZnO nanorods by simple and cost effective 2-step hydrothermal method. The fabrication of sensor from ZnO nanorods was used for ethanol gas sensing at low temperature and results are in agreement with an earlier study. The results showed that oxygen absorption and desorption can illustrates the present of defects that are useful for gas sensing process. It was investigated from the experimental results that sensor shows a maximum response at 80°C for ethanol. The sensitivity of the sensor to ethanol depends upon the lengths of nanorods and also increased with increasing concentration of ethanol vapor, humidity as well as temperature. It was investigated that sensor has stable response (%) and recovery time at 80°C to ethanol. The fabricated sensor was also used to test the hydrogen gas at mild temperature conditions i.e. 25, 30 and 50°C. Resistance of the sensor decreased with the induction of hydrogen gas and attains the same resistance values with the ejection of the gas. It was also investigated that with the increase in temperature resistance of hydrogen gas decreases. Moreover, the experimental results revealed that the sensing hydrogen gas at 50°C show a maximum sensitivity of 20.

Acknowledgement

The authors would like acknowledged and thankful to Higher Education Commission of Pakistan (HEC) for the financial support to International Research Support Initiative Programme (IRSIP), Material and Metallurgy Department of the Cambridge University to utilized their

research facilities like XRD, SEM, UV spectrometer, gas sensing equipment and centre for nanotechnology Physics Department University of the Punjab.

References

[1] S. Q. Zhao, L. M. Yang, W. W. Liu, K. Zhao, Y. L. Zhou and Q. L. Zhou, Chin. Phys. B. **19**, 08720 (2010)
[2] X. M. Chen, J. Yong, X. Y. Gao, and X. W. Zhao, Chin. Phys. B. **21**, 116801 (2012)
[3] X. B. He, T. Z. Yang, J. M. Cai, C. D. Zhang, H. M. Guo, D. X. Shi, C. M. Shen, H. J. Gao, Chin. Phys. Soc.17 (2008)
[4] Rajesh Kumar, Girish Kumar, and Ahmad Umar Nanosci. Nanotechnol. Lett. **6**, 631 (2014)
[5] L. Ming, H. Y. Zhang, C. X. Guo, J. B. Xu, X. J. Fu, and P. F. Chen, Chin. Phys. Soc. 18 (2009)
[6] G. C. Yi, W. Chunrui and P. Won Il, Semicond. Sci. Technol. **20**, 22 (2005)
[7] D. Appell, Nanotechnol. Wired for success Nature **419**, 553 (2002)
[8] K. Mirabbaszadeh and M. Mehrabian, Phys. Scr. **85**, 035701 (2012)
[9] X. Y. Teng, Y. H. Wu, W. Yu, W. Gao, G. S. Fu, Chin. Phys. B. **21**, 097105 (2012)
[10] S.S. Li, Z. Zhang, J. Z. Huang, X. P. Feng and R. X. Liu, Chin. Phys. B. **20**, 127102 (2011)
[11] X. F. Duan, Y. Huang, Y. Cui, J. F. Wang and C. M. Lieber, Nature **409**, 66 (2001)
[12] O. Lupan, C. Guangyu, C. Lee, Microelectronics Journal. **38,** 1211 (2007)
[13] W. T. Seeber, M. O. Abou-Helal, S. Barth, D. Beil, T. Hoche, H. H. Afify, S. E. Demian, Mat. Sci. Semicon. Proc. **2**, 45 (1999)
[14] L. Samuelson, Mater.Today. **6**, 22 (2003)
[15] O. Lupana, L. Chow, Th. Pauporté, L. K. Ono, B. Roldan Cuenya, G. Chai, Sensors and Actuators B. **173**, 772 (2012)
[16] Z. L. Wang, J. Phys. Condens. Matte. **16**, 829 (2004)
[17] C. H. Liu, B. C. Liu and Z. X. Fu, Chin. Phys. B. **17**, 2292 (2008)
[18] W. Mingsong, K. Eui, J. S. Chung, E. W. Shin, H. H. Sung, K. E. Lee, P. Chinho, phys. stat. sol. **203**, 2418 (2006)
[19] L. P. Peng, L. Fang, W. D. Wu, X. M. Wang, L. Li, Chin. Phys. B. **21**, 047305 (2012)
[20] R. J. Hong, X. Jiang, G. Heide, B. Szyszka, V. Sittinger, S. H. Xu, W. Werner, G. Heide, J. Cryst. Growth. **249**, 461 (2003)
[21] X. Q. Wei, B. Y. Man, M. Liu, C. S. Xue, H. Z. Zhuang, C. Yang, Physica B. **388**, 145 (2007)
[22] C. Chen, Y. Ji, X. Y. Gao, M. K. Zhao, J. M. Ma, Z. Y. Zhang and J. X. Lu, Acta Phys. Sin. **61**, 036104 (2012)
[23] N. Ueno, T. Maruo, N. Norikazu, Y. Egashira, K. Ueyama, Mater. Lett. **64**, 513 (2010)
[24] D. X. Tang and Y. Zhao, Chin. J. Chem. Phys. **16**, 237 (2003)
[25] X. Y. Zhao, C. Z. Li, B. C. Zheng, H. C. Gu and L. M. Hu, J. of East China University of Sci. and Technol. **23**, 191 (1997)
[26] M. M. Lu, X. M. Ma and W. J. Cheng, J. Synth. Cryst. **38**, 870 (2009)
[27] O. Lupan, G. Chaic, L. Chow, Microelectronic Eng. **85**, 2220 (2008)
[28] S. T. Shishiyanua, O. I. Lupan, E. V. Monaico, V. V. Ursaki, T. S. Shishiyanu, I. M. Tiginyanu, Thin Solid Films. **488**(1-2), 15 (2005)
[29] C. C. Lin and Y. Y. Li, Materials Chem. and Phys. **113**, 334 (2009)
[30] W. Mingsong, E. J. Kim, J. S. Chung, E. W. Shin, H. H. Sung, K. E. Lee, and P. Chinho, phys. stat. sol. **203**, 2418 (2006)
[31] S. Bandyopadhyay, G. K. Paul, R. Roy, S. K. Sen, and S. Sen, Mater. Chem. Phys. 74, (2002)
[32] S. Uthanna, T. K. Subramanyam, B. S. Naidu, and G. M. Rao, Opt. Maer. 19, (2002)
[33] K. Mirabbaszadeh and M. Mehrabian, Phys. Scr. **85**, 035701 (2012)
[34] M. Amin, U. Manzoor, M. Islam, A. S. Bhatti and N. A. Shah, Sensors. **12**, 13842 (2012)
[35] L. W. Zhong, J. Phys. Condens. Matter. **16**, 829 (2004)
[36] M. Li, H. Y. Zhang, C. X. Guo, J. B. Xu, X. J. Fu, and P. F. Chen, Chin. Phys. Soc.

18, (2009)
[37] T. J. Hsueh, C. L. Hsu, Sensors and Actuators B. **131**, 572 (2008)
[38] N. Barsan, M. Schweizer-Berberich, W. Gopel, Fresenius, J. Anal. Chem. **365**, 287 (1999)
[39] O. Lupan, V. V. Ursaki, G. Chaic, L. Chow, G. A. Emelchenko, I. M. Tiginyanu, A. N. Gruzintsev, A. N. Redkin, Sensors and Actuators B: Χημιχαλ. **144**(1), 56 (2010)